Research Article

Methodology Design to Predict the Solidification Process of Pure Water inside Cylindrical Enclosure

Adil A. Alwan[#][*] and Rafel H. Hameed[#]

[#]Department of Mechanical Eng., College of Eng., University of Babylon, Iraq, Babylon

Abstract

A computational methodology was simulated to determine the spatial and temporal temperature profile within each phase and phase change location by assuming the heat transfer in both phases is by pure conduction in order to demonstrate the mechanism of solidification process inside close cylindrical enclosure. ADI algorithm was used to promote the mathematical model for solidification depending upon assumption of the position of heat flux from the down, and the diameter value of cylindrical enclosure. This method gave a good solution and damping the oscillation errors with along computing time.

Keywords: solidification, phase change mechanism, ADI

1. Introduction

Phase change in cylindrical geometry is of great interest both from the theoretical point of view and for practical applications, including casting and development of heat storage system based on the use of latent heat. The solution of moving boundary problems with phase changes has been of special interest due to the inherent difficulties associated with the nonlinearity of the interface conditions and the unknown locations of phase change problems are available only for a limited number of cases. (Tszeng *et al*, 1989) developed a mathematical modeling technique which is able to solve the heat transfer problem associated with the phase change in solidification.

A temperature recovery method was proposed to handle the latent heat generation for both the cases of congruent solidification and mushy-zone solidification. This scheme was implemented in a nonlinear finite element program by which numerical calculation has been carried out. The results showed good agreement with the available analytical solution. Conducted an experimental study of the freezing and melting processes for water contained in spherical elements. (Eames and Adref, 2002) revealed quantitative data on the movement of the solid-liquid interface position with time, the effect of heat transfer fluid (coolant) temperature, and the effect of sphere size on the melting and freezing processes. They also showed the discharge and charge rate and time required to melt and freeze a spherical ice storage element. Finally, their

results were used to derive empirical equations describing charge and discharge for an ice storage element. (Michalek and Kowalewski, 2003) analyzed three numerical benchmarks concerning the freezing of water using the commercial Fluent code. The first case is a steady-state natural convection in a different heated cavity for temperature near the freezing point. In the second case, the freezing of water in a different heated cavity is simulated. The third case describes a simulation of freezing water in the presence of forced convection and a free surface flow. Two finite-differences numerical codes are used to verify the results of the Fluent simulation for the natural convection and solidification in the different heated cavity. It is found that the simulation of water solidification requires very fine meshes and short time steps, extending the computational time of the extreme. (Stampa and Nieckele, 2004) investigated numerically the charging process behavior occurring in a typical indirect ice storage tank. It consists of analyzing the heat transfer and removal of energy applicable to storage systems which are chiller-based.

In this sense the secondary coolant circulates through a heat exchanger that is submerged in a tank of water and it is used to freeze (charge) the phase-change material (water) which never leaves the storage tank. The thermal exchange process is investigated considering the storage tank in two different positions. In the first one the storage tank is in the vertical position, while for the second, it is horizontally positioned. The storage tank is represented by a channel formed by parallel flat plates, one of which is the heat exchanger. The results are analysed through streamlines and isotherms, for

*Corresponding author: **Adil A. Alwan**

specific instants of time. The heat transfer effectiveness, the average heat flux and solid formed at one of the two plates of the channel are compared with the vertical and horizontal positions of the channel. (Alawadhi, 2004) studied numerically the unsteady natural convection flow during freezing of pure water in a circular enclosure using ANSYS. Mathematical model for solidification process is based on apparent capacity method and viscosity depends on temperature formulation. The governing equations are discretized on a fixed grid. Water's temperature is initially higher than its freezing temperature $T_o=21$ ℃. Then, the temperature of the enclosure's boundary is dropped to -10 ℃. Ice forms at the enclosure boundary while natural convection flow is induced in the liquid region. Calculations have been made for the rate of the change of the solid fraction and flow field, and density inversion near freezing temperature phenomenon of water is considered. The results are validated with previously published experimental data, and a good agreement is found. (Alrmah, 2005) investigated the finite element solution of solidification process in 2-D Cartesian and axisymmetric geometries. The use of finite element may result in spurious increase of temperature in the field and the selection of the mushy zone range when used as a numerical tool along with the selection of the mesh size results in large errors in the predicted solidification time. The approach works best for problems where the mushy zone range is finite and the thermal conductivities of both phases are high. (Buyruk *et al*, 2009) calculated numerically the effect of ice formation on different cylinder geometries placed in a rectangular ice storage tank filled with water. Fluent package program was used for numerical solution of flow domain to depict temperature distribution and ice formation. Water temperature in tank and cylinder surface temperature were assumed as 4 ℃ and -10 ℃ respectively. Temperature distribution, liquid fraction and ratio of Ai/Ac (formed ice area / cross sectional area of cylinder) were determined for various cylinder geometries. (Ezan *et al*, 2011) investigated numerically solidification process inside a water filled rectangular cavity. The mathematical model is validated by comparing the numerical model predicted with the available analytical, numerical, and experimental results for three different test cases: one-dimensional conduction dominated solidification, natural convection in rectangular cavity, and natural convection dominated solidification in rectangular cavity. For all three cases, some good agreements are achieved in terms of isotherms, interface positions, and streamlines. After validation, time-wise ice formations are represented, and comparisons are made between bare and finned wall cases. In addition to these, further analyses are carried out by neglecting the buoyancy force to introduce the differences between natural convection dominated and conduction dominated models. The results emphasize that natural convection has a critical effect in actual phase change processes.

2. Mathematical Model

It has been used a cylindrical coordinates approach to portend the temperature distribution inside the cylindrical rig to explicate the phase change phenomena of working fluid (pure water). The working fluid was changed from liquid phase to solid phase due to the location of melting point. The solidification process (freezing), which was heat conduction problem involving a phase change. This is also called moving boundary problem because of the unexplored moving liquid-solid interface. The moving boundary problem is greatly non-linear and it is rendered more intricate. If the involved thermo-physical properties are temperature dependent, which also makes each problem somewhat unique. A 3-dimensional in polar coordinates heat conduction equation was used to cover this phenomenon. This equation was given by (Karlekar and Desmond, 1982).

$$\rho\, c_p\, \frac{\partial T}{\partial t} = k\frac{\partial^2 T}{\partial r^2} + k\frac{1}{r}\frac{\partial T}{\partial r} + k\frac{1}{r^2}\frac{\partial^2 T}{\partial \theta^2} + k\frac{\partial^2 T}{\partial z^2} \qquad (1)$$

Assuming that the thermal properties are independent of temperature, the working fluid is taken to be homogenous and isotropic, equation (1) reduced to

$$\frac{1}{\alpha}\frac{\partial T}{\partial t} = \frac{\partial^2 T}{\partial r^2} + \frac{1}{r}\frac{\partial T}{\partial r} + \frac{1}{r^2}\frac{\partial^2 T}{\partial \theta^2} + \frac{\partial^2 T}{\partial z^2} \qquad (2)$$

Where $\alpha = \frac{k}{\rho\, c_p}$

(Adams and Rogers, 1973) exhibited that the cylinder is solid rather than hollow, special attention must be given to the middle node at r = 0. At r = 0 the second expression in equation (2), $(\frac{1}{r}\frac{\partial T}{\partial r})$ is indeterminate. This term can be evaluated by using L'Hopital's rule. Then, the governing partial differential equation at r = 0 can be penned

$$\frac{\partial^2 T}{\partial r^2} + \frac{\partial^2 T}{\partial r^2} + \frac{\partial^2 T}{\partial z^2} = \frac{1}{\alpha}\frac{\partial T}{\partial t} \qquad (3)$$

A further two dimensional model of partial significance is two dimensional transient conduction in the radial and axial direction. For T = T(r, z, t), and equation (2) reduces to:

$$\frac{\partial^2 T}{\partial r^2} + \frac{1}{r}\frac{\partial T}{\partial r} + \frac{\partial^2 T}{\partial z^2} = \frac{1}{\alpha}\frac{\partial T}{\partial t} \qquad (4)$$

Equations (2) and (4) were a heat equations which were classified as a parabolic partial differential equations, isotropic medium.

Cylindrical domain was used in solving theoretically the task of solidification in two zones separated by phase change (liquid zone and solid zone). This heat flux was used to remove the heat through the solidification process. In the first approach the heat flux was fixed from the down of cylindrical domain with assumptions of dimensions and the position of interface line as shown in figure (1).

The initial and boundary conditions were assumed as noted in figure (2). Initial temperature of working fluid (pure water) T_o = 24 °C at initial time t = 0 as: $T(r, z, 0) = T_o$
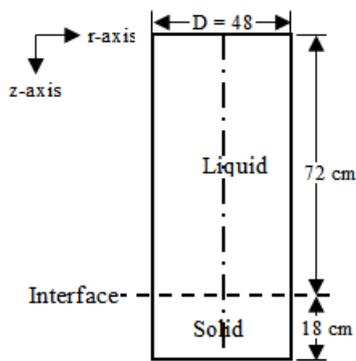

Fig.1 Schematic diagram of assumption

The boundary conditions as:

at z = L= 90 , $-k\frac{\partial T}{\partial z} = \bar{\bar{q}}$ (heat flux)

at r = R , $\frac{\partial T}{\partial r} = 0$ (insulation)

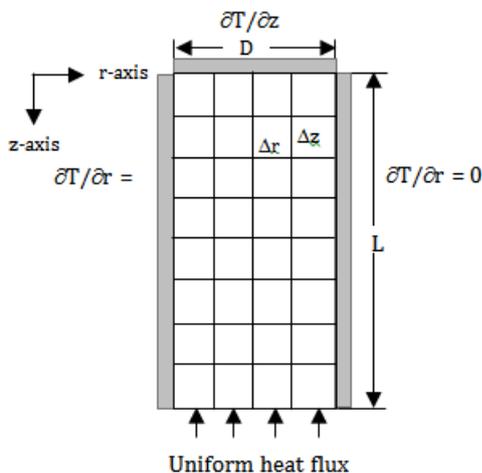at z = 0 , $\frac{\partial T}{\partial z} = 0$ (insulation)

Fig.2 Grid layout for cylinder

3. Numerical Solution Technique

It has been assumed a half domain of cylinder to design the model, this is due to the symmetrical shape of rig, and the water was homogenous. The grid is represented by figure (3). The mesh nodes number are 25×91, the distance in between points in the established grid are Δr, Δz, and Δt. Numerical simulations have been performed with the ADI (Alternating Direction Implicit) method. (Anderson *et al*, 1984) demonstrated that the challenges, which occur when attempting to decipher the 2-D heat equation by ordinary algorithms, guided to the advance of alternating-direction implicit (ADI) method.

The typical ADI method is a two-step scheme granted by

Step1: $\frac{T_{i,j}^{n+1/2}-T_{i,j}^{n}}{\Delta t/2} = \alpha \left(\frac{T_{i+1,j}^{n+1/2}-2T_{i,j}^{n+1/2}+T_{i-1,j}^{n+1/2}}{\Delta x^2} + \frac{T_{i,j+1}^{n}-2T_{i,j}^{n}+T_{i,j-1}^{n}}{\Delta y^2} \right)$

(5)

Step 2:

$\frac{T_{i,j}^{n+1}-T_{i,j}^{n+1/2}}{\Delta t/2} = \alpha \left(\frac{T_{i+1,j}^{n+1/2}-2T_{i,j}^{n+1/2}+T_{i-1,j}^{n+1/2}}{\Delta x^2} + \frac{T_{i,j+1}^{n+1}-2T_{i,j}^{n+1}+T_{i,j-1}^{n+1}}{\Delta y^2} \right)$ (6)
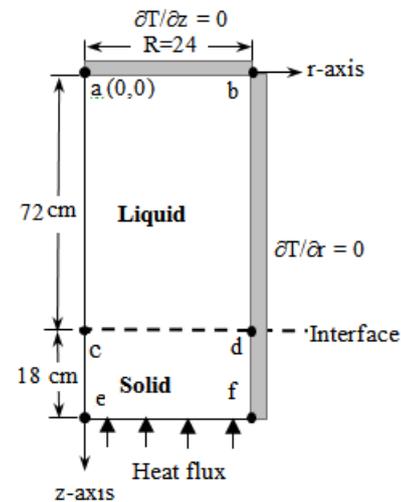

Fig.3 Two-dimensional computational mesh

Accordingly of the "splitting" which is utilized in this algorithm, just tridiagonal systems of linear algebraic equations must be uncovered. Through level 1, a tridiagonal matrix is solved for each j row of grid points and amid level 2, a tridiagonal matrix is settled for every i row of grid points. The ADI method is second-order precise with a truncation error of O [$(\Delta t)^2$, $(\Delta x)^2$, $(\Delta y)^2$].

It has been shown that the ADI method gave more reliable results and stability analysis than other method. Apply ADI algorithm to investigate how the cooling and freezing of idle water in cylindrical domain under the boundary conditions which were assumed and from the initial temperature of water to its freezing point

The time needed to cool the water from its beginning temperature to the freezing point can be established by considering a two-dimensional transient heat conduction model in cylindrical coordinates. It was assumed Δr = Δz = 2 cm. Then, the mesh nodes number are 46 × 13, producing a tridiagonal matrix 598 row × 598 column of grid points. That was needed time as seven and a half hours to simulate the phase change starting inside the enclosure. It was predicted that the phase change at 18 cm from the down of enclosure, and with time of 180 minutes. The prediction model was simulated the liquid-solid phase change phenomenon for stagnant water in cylindrical enclosure.

3.1 Temperature Distribution through Liquid Phase

In liquid phase the transient heat equation in two-dimension polar coordinates provides more constancy to compute the temperature prorating in two-dimension domain of the limit space assembly until the phase change happens at interface line as shown in figure (3). It is assumed at the 18 cm from the heat flux supply. The temperature of liquid is reduced from the initial temperature to saturated temperature (freezing point) at this interface line. That connotes the solidification phenomena is take place. The computer program goal to give more durability to compute the temperature profile against r and z coordinates depending upon the boundary conditions. After represented these equations by ADI scheme. All the points lying on the boundary a-b-d-e-f are called boundary nodes, and the rest of the points of the grid are called internal nodes.

a-Temperature Distribution at Point a

$$\text{Step 1:} -\frac{\lambda}{2} T_{i+1,j}^{n+1/2} + \left(1 + \frac{\lambda}{2}\right) T_{i,j}^{n+1/2} = \frac{\lambda}{2} T_{i,j+1}^n + \left(1 - \frac{\lambda}{2}\right) T_{i,j}^n \tag{7}$$

$$\text{Step 2:} -\frac{\lambda}{2} T_{i,j+1}^{n+1} + \left(1 + \frac{\lambda}{2}\right) T_{i,j}^{n+1} = \frac{\lambda}{2} T_{i+1,j}^{n+1/2} + \left(1 - \frac{\lambda}{2}\right) T_{i,j}^n \tag{8}$$

Where $\lambda = \frac{\alpha_L \Delta t}{\Delta r^2}$

b-Temperature Distribution through r-axis

$$\text{Step 1:} -\frac{\lambda}{4} T_{i+1,j}^{n+1/2} + \left(1 + \frac{\lambda}{2}\right) T_{i,j}^{n+1/2} - \frac{\lambda}{4} T_{i-1,j}^{n+1/2} = \frac{\lambda}{2} T_{i,j+1}^n + \left(1 - \frac{\lambda}{2}\right) T_{i,j}^n \tag{9}$$

$$\text{Step 2:} -\frac{\lambda}{2} T_{i,j+1}^{n+1} + \left(1 + \frac{\lambda}{2}\right) T_{i,j}^{n+1} = \frac{\lambda}{4} T_{i+1,j}^{n+1/2} + \left(1 - \frac{\lambda}{2}\right) T_{i,j}^{n+1/2} + \frac{\lambda}{4} T_{i-1,j}^{n+1/2} \tag{10}$$

Applying energy balance for corner node b as boundary node, where r = R, and z = 0, then the ADI scheme for this corner node b was constructed as:

$$\text{Step 1:} -\frac{\lambda}{4} T_{i-1,j}^{n+1/2} + \left(1 + \frac{\lambda}{2}\right) T_{i,j}^{n+1/2} = \frac{\lambda}{4} T_{i,j+1}^n + \left(1 - \frac{\lambda}{4}\right) T_{i,j}^n \tag{11}$$

$$\text{Step 2:} -\frac{\lambda}{4} T_{i,j+1}^{n+1} + \left(1 + \frac{\lambda}{4}\right) T_{i,j}^{n+1} = \frac{\lambda}{4} T_{i-1,j}^{n+1/2} + \left(1 - \frac{\lambda}{4}\right) T_{i,j}^{n+1/2} \tag{12}$$

c-Temperature Distribution through z-axis

To simulate the temperature distribution through z-axis in liquid phase where r = 0, and the length of z < interface line, which means to sweep i = 1 to 1, and j = 2 to 72.

$$\text{Step 1:} -2\lambda T_{i+1,j}^{n+1/2} + (1 + 2\lambda) T_{i,j}^{n+1/2} = \frac{\lambda}{2} T_{i,j+1}^n + (1 - \lambda) T_{i,j}^n + \frac{\lambda}{2} T_{i,j-1}^n \tag{13}$$

$$\text{Step 2:} -\frac{\lambda}{2} T_{i,j+1}^{n+1} + (1 + \lambda) T_{i,j}^{n+1} - \frac{\lambda}{2} T_{i,j-1}^{n+1} = 2\lambda T_{i+1,j}^{n+1/2} + (1 - 2\lambda) T_{i,j}^{n+1/2} \tag{14}$$

e-Temperature Distribution through r-z Plane

$$\text{Step1:} -\left(\frac{\lambda}{2} + \frac{\lambda 1}{4}\right) T_{i+1,j}^{n+1/2} + (1 + \lambda) T_{i,j}^{n+1/2} - \left(\frac{\lambda}{2} - \frac{\lambda 1}{4}\right) T_{i-1,j}^{n+1/2} = \frac{\lambda}{2} T_{i,j+1}^n + (1 - \lambda) T_{i,j}^n + \frac{\lambda}{2} T_{i,j-1}^n \tag{15}$$

$$\text{Step2:} -\frac{\lambda}{2} T_{i,j+1}^{n+1} + (1 + \lambda) T_{i,j}^{n+1} - \frac{\lambda}{2} T_{i,j-1}^{n+1} = \left(\frac{\lambda}{2} + \frac{\lambda 1}{4}\right) T_{i+1,j}^{n+1/2} + (1 - \lambda) T_{i,j}^{n+1/2} + \left(\frac{\lambda}{2} - \frac{\lambda 1}{4}\right) T_{i-1,j}^{n+1/2} \tag{16}$$

For energy balance at the end of r-z plane in liquid phase. These nodes are a boundary nodes which were insulated. For r = R to L, and z = 2 to 72. Then, the ADI scheme represented as:

$$\text{Step 1:} -\frac{\lambda}{2} T_{i-1,j}^{n+1/2} + \left(1 + \frac{\lambda}{2}\right) T_{i,j}^{n+1/2} = \frac{\lambda}{2} T_{i,j+1}^n + \left(1 - \frac{\lambda}{2}\right) T_{i,j}^n + \frac{\lambda}{4} T_{i,j-1}^n \tag{17}$$

$$\text{Step 2:} -\frac{\lambda}{4} T_{i,j+1}^{n+1} + \left(1 + \frac{\lambda}{2}\right) T_{i,j}^{n+1} - \frac{\lambda}{4} T_{i,j-1}^{n+1} = \left(1 - \frac{\lambda}{2}\right) T_{i,j}^{n+1/2} + \frac{\lambda}{2} T_{i-1,j}^{n+1/2} \tag{18}$$

3.2. Temperature Distribution at Interface Line cd

Where the energy-balance equation of the interface will be

$$k_s \frac{\partial T_s}{\partial z} - k_L \frac{\partial T_L}{\partial z} = \rho L \frac{\partial \delta(t)}{\partial t}, \text{ at } z = \delta(t) \tag{19}$$

From the interface energy-balance at z = δ (t) for solidification process equation (19)

$$-k_L \frac{\partial T}{\partial z} = \rho L \frac{\partial \delta(t)}{\partial t}, \text{ at } z = \delta(t) \tag{20}$$

This is the moving boundary condition (M.B.C), which uses in heat equation to simulate the temperature distribution through the phase change where $\frac{\partial \delta(t)}{\partial t}$, the velocity of interface in position of z-axis direction is

$$\frac{\partial \delta(t)}{\partial t} = V_*, \text{ at } z = \delta (t) \tag{21}$$

Then, the moving boundary condition is represented as

$$-k_L \frac{\partial T}{\partial z} = \rho L V_*, \text{ at } z = \delta(t) \tag{22}$$

Where L is the specific latent heat of solidification, and V_* is the velocity of solidification (phase change). In this approach the phase change is assumed to start at distance 18 cm from the position of heat flux supply. (Alwan, 2002) illustrate that the velocity of phase change into solidification process is given by the expression

$$\frac{d\delta(t)}{dt} = V_* = \frac{\text{heat flux}}{[\rho_L L + \rho_L c_{pL}(T_L - T_s)]} \tag{23}$$

a-Phase change at point c

This point on the domain surface is considered the starting of phase change as noted in figure (3). The interface line between liquid and solid phase change is assumed to be propagated through r-axis. The finite difference form of equation (22) is written as:

$$-k_L \frac{T_{i,j+1} - T_{i,j-1}}{2\Delta z} = \rho L V_* \tag{24}$$

$$T_{i,j-1} = T_{i,j+1} + \frac{\rho L V_* 2\Delta Z}{k_L} \tag{25}$$

$$T_{i,j}^{n+1} = 4\lambda T_{i+1,j}^n - 4\lambda T_{i,j}^n + \lambda T_{i,j+1}^n - 2\lambda T_{i,j}^n + \lambda T_{i,j-1}^n + T_{i,j}^n \tag{26}$$

Where $\lambda = \frac{\alpha_L \Delta t}{\Delta r^2}$

Then, substituting the dynamic boundary condition of equation (25) into equation (26) as:

$$T_{i,j}^{n+1} = 4\lambda T_{i+1,j}^n - 4\lambda T_{i,j}^n + \lambda T_{i,j+1}^n - 2\lambda T_{i,j}^n + \lambda \left[T_{i,j+1}^n + \frac{\rho L V_* 2\Delta z}{k_L} \right] + T_{i,j}^n \tag{27}$$

Represented the ADI scheme to equation (26), this equation becomes as:

Step 1: $-2\lambda T_{i+1,j}^{n+1/2} + (1+2\lambda) T_{i,j}^{n+1/2} = \lambda T_{i,j+1}^n + (1-\lambda)T_{i,j}^n + \frac{\lambda}{2} \frac{\rho L V_* 2\Delta z}{k_L}$ (28)

Step 2: $-\lambda T_{i,j+1}^{n+1} + (1+\lambda)T_{i,j}^{n+1} = 2\lambda T_{i+1,j}^{n+1/2} + (1-2\lambda)T_{i,j}^{n+1/2} + \frac{\lambda}{2}\frac{\rho L V_* 2\Delta z}{k_L}$ (29)

b-Phase change through r-axis

Step 1: $-\left(\frac{\lambda}{2} + \frac{\lambda 1}{4}\right) T_{i+1,j}^{n+1/2} + (1+\lambda)T_{i,j}^{n+1/2} - \left(\frac{\lambda}{2} - \frac{\lambda 1}{4}\right) T_{i-1,j}^{n+1/2} = \lambda T_{i,j+1}^n + (1-\lambda)T_{i,j}^n + \frac{\lambda}{2}\frac{\rho L V_* 2\Delta z}{k_L}$ (30)

Step 2: $-\lambda T_{i,j+1}^{n+1} + (1+\lambda)T_{i,j}^{n+1} = \left(\frac{\lambda}{2} + \frac{\lambda 1}{4}\right) T_{i+1,j}^{n+1/2} + (1-\lambda)T_{i,j}^{n+1/2} + \left(\frac{\lambda}{2} - \frac{\lambda 1}{4}\right) T_{i-1,j}^{n+1/2} + \frac{\lambda}{2}\frac{\rho L V_* 2\Delta z}{k_L}$ (31)

Where $\lambda 1 = \frac{\alpha_L \Delta t}{\Delta r\, r_i}$

Also, simulated the phase change at the end of r-axis as a boundary condition, which was insulated. That means r = R, and z = 73. Then energy balance at point d was done, and represented by ADI scheme as:

Step 1: $-\frac{\lambda}{2} T_{i-1,j}^{n+1/2} + \left(1+\frac{\lambda}{2}\right) T_{i,j}^{n+1/2} = \frac{\lambda}{2} T_{i,j+1}^n + \left(1-\frac{\lambda}{2}\right) T_{i,j}^n + \frac{\lambda}{4}\frac{\rho L V_* 2\Delta z}{k_L}$ (32)

Step 2: $-\frac{\lambda}{2} T_{i,j+1}^{n+1} + \left(1+\frac{\lambda}{2}\right) T_{i,j}^{n+1} = \frac{\lambda}{2} T_{i-1,j}^{n+1/2} + \left(1-\frac{\lambda}{2}\right) T_{i,j}^{n+1/2} + \frac{\lambda}{2}\frac{\rho L V_* 2\Delta z}{k_L}$ (33)

3.3 Temperature Distribution through Solid Phase

When liquid assuming to be changed to solid phase after the interface line. The transient heat equation is used to predict the temperature distribution through solid phase, point 74 in domain of enclosure is assumed in solid phase, i.e. z > interface line

a- Temperature distribution through z-axis

Step 1: $-2\lambda T_{i+1,j}^{n+1/2} + (1+2\lambda)T_{i,j}^{n+1/2} = \frac{\lambda}{2} T_{i,j+1}^n + (1-\lambda)T_{i,j}^n + \frac{\lambda}{2} T_{i,j-1}^n$ (34)

Step 2: $-\frac{\lambda}{2} T_{i,j+1}^{n+1} + (1+\lambda)T_{i,j}^{n+1} - \frac{\lambda}{2} T_{i,j-1}^{n+1} = 2\lambda T_{i+1,j}^{n+1/2} + (1-2\lambda)T_{i,j}^{n+1/2}$ (35)

Where $\lambda = \frac{\alpha_s \Delta t}{\Delta r^2}$ and $\lambda 1 = \frac{\alpha_s \Delta t}{\Delta r\, r_i}$. That means the thermal properties of water in solid case were used.

b-Temperature distribution through r-z plane

Step 1: $-\left(\frac{\lambda}{2} + \frac{\lambda 1}{4}\right) T_{i+1,j}^{n+1/2} + (1+2\lambda)T_{i,j}^{n+1/2} - \left(\frac{\lambda}{2} - \frac{\lambda 1}{4}\right) T_{i-1,j}^{n+1/2} = \frac{\lambda}{2} T_{i,j+1}^n + (1-\lambda)T_{i,j}^n + \frac{\lambda}{2} T_{i,j-1}^n$ (36)

Step 2: $-\frac{\lambda}{2} T_{i,j+1}^{n+1} + (1+\lambda)T_{i,j}^{n+1} - \frac{\lambda}{2} T_{i,j-1}^{n+1} = \left(\frac{\lambda}{2} + \frac{\lambda 1}{4}\right) T_{i+1,j}^{n+1/2} + (1-2\lambda)T_{i,j}^{n+1/2} + \left(\frac{\lambda}{2} - \frac{\lambda 1}{4}\right) T_{i-1,j}^{n+1/2}$ (37)

It has been used energy balance at the end of r-z plane in solid phase. It was done to simulate the temperature of the boundary nodes at r = R, and z >74 as shown in figure (3). Then, used ADI scheme as:

Step 1: $-\frac{\lambda}{2} T_{i-1,j}^{n+1/2} + \left(1+\frac{\lambda}{2}\right) T_{i,j}^{n+1/2} = \frac{\lambda}{4} T_{i,j+1}^n + \left(1-\frac{\lambda}{2}\right) T_{i,j}^n + \frac{\lambda}{4} T_{i,j-1}^n$ (38)

Step 2: $-\frac{\lambda}{4} T_{i,j+1}^{n+1} + \left(1+\frac{\lambda}{2}\right) T_{i,j}^{n+1} - \frac{\lambda}{4} T_{i,j-1}^{n+1} = \frac{\lambda}{2} T_{i-1,j}^{n+1/2} + \left(1-\frac{\lambda}{2}\right) T_{i,j}^{n+1/2}$ (39)

c-Temperature distribution through line ef

At the down line ef, which was the heat flux fixed. It has been used the energy balance to calculate the temperature for these nodes at boundary. Then applied ADI scheme for different steps. Firstly, at the center point e in figure (3), that mean r = 0, and z = M.

Step 1: $-\frac{\lambda}{2} T_{i+1,j}^{n+1/2} + \left(1+\frac{\lambda}{2}\right) T_{i,j}^{n+1/2} = \frac{\lambda}{2} T_{i,j-1}^n + \left(1-\frac{\lambda}{2}\right) T_{i,j}^n - \frac{\bar{q}\Delta r\,\Delta t}{4\,\rho_s\, c_{p_s}}$ (40)

Step 2: $-\frac{\lambda}{2} T_{i,j-1}^{n+1} + \left(1+\frac{\lambda}{2}\right) T_{i,j}^{n+1} = \frac{\lambda}{2} T_{i+1,j}^{n+1/2} + \left(1-\frac{\lambda}{2}\right) T_{i,j}^{n+1/2} - \frac{\bar{q}\Delta r\,\Delta t}{4\,\rho_s\, c_{p_s}}$ (41)

Secondly balance energy for boundary nodes through r-axis. That means r > 0, and z = M. for i = 2 to L-1 and j = M to M, and applied the ADI scheme as:

Step 1: $-\frac{\lambda}{4}T_{i+1,j}^{n+1/2} + \left(1+\frac{\lambda}{2}\right)T_{i,j}^{n+1/2} - \frac{\lambda}{4}T_{i-1,j}^{n+1/2} = \frac{\lambda}{2}T_{i,j-1}^{n} + \left(1-\frac{\lambda}{2}\right)T_{i,j}^{n} - \frac{\bar{\bar{q}}\,\Delta r\,\Delta t}{4\,\rho_s\,c_{p_s}}$ (42)

Step 2: $-\frac{\lambda}{2}T_{i,j-1}^{n+1} + \left(1+\frac{\lambda}{2}\right)T_{i,j}^{n+1} = \frac{\lambda}{4}T_{i+1,j}^{n+1/2} + \left(1-\frac{\lambda}{2}\right)T_{i,j}^{n+1/2} - \frac{\bar{\bar{q}}\,\Delta r\,\Delta t}{4\,\rho_s\,c_{p_s}}$ (43)

Finally, the energy balance was done at the corner f. This point is a boundary node as shown in figure (3), for i = L to L , and j = M to M, and used ADI scheme as:

Step 1: $-\frac{\lambda}{4}T_{i-1,j}^{n+1/2} + \left(1+\frac{\lambda}{4}\right)T_{i,j}^{n+1/2} = \frac{\lambda}{4}T_{i,j-1}^{n} + \left(1-\frac{\lambda}{4}\right)T_{i,j}^{n} - \frac{\bar{\bar{q}}\,\Delta r\,\Delta t}{8\,\rho_s\,c_{p_s}}$ (44)

Step 2: $-\frac{\lambda}{4}T_{i,j-1}^{n+1} + \left(1+\frac{\lambda}{4}\right)T_{i,j}^{n+1} = \frac{\lambda}{4}T_{i-1,j}^{n+1/2} + \left(1-\frac{\lambda}{4}\right)T_{i,j}^{n+1/2} - \frac{\bar{\bar{q}}\,\Delta r\,\Delta t}{8\,\rho_s\,c_{p_s}}$ (45)

4. Results and Discussion

This approach was designed as a cylindrical enclosure with assumption the heat flux was placed from down of inside part of cylinder, and the domain dimensions of enclosure were 48 cm of diameter and the length 90 cm. Upon the boundary conditions assumption which were assumed all the sides part and top part perfectly insulation to prevent the heat losses of test enclosure. Upon these assumptions the methodology was simulated and numerical analyses are performed to predict the temperature distribution inside the domain of enclosure to explain the phase change phenomenon of pure water as moving boundary problem.

Figure (4) shows the temperature distribution through z-axis at r = 0 with different interval time of 60 minutes through solidification process. It has been shown the function response of temperature at the layer less than 40 cm still appear at constant temperature. That means reduction in temperature from the ambient very low. Also, this figure indicates that the phase change not happened before 180 minutes as pointed in response function of temperature distribution at time 60 and 120 minutes. This figure also explains that when the time of freezing increasing the location of phase change upward moving of water layer. This moving very slowly and takes along times.

Figure (5) represents the phase change line temperature which was about 0.01 to 0.05 °C, which means around freezing point 0 °C. This location of phase change line predicted at 180 minutes, and at z = 72 cm in the domain of cylindrical enclosure. This results consistent with work of (Scanlon and Stickl, 2004). It has been assumed in this model that latent heat of water is taken to be 333 kJ/kg and ∆T was set to be 0.04 °C. The phase change calculate in this model which solved by ADI method. It was taken moving boundary condition, and occurs variation in thermo physical properties and density of water in solid phase. (Ulvrov *et al*, 2012) show at the phase change interface a jump in the heat flux corresponding to the release of latent heat. This jump indicates by the velocity of phase change, which was calculated in this model about 0.000003 m/s.
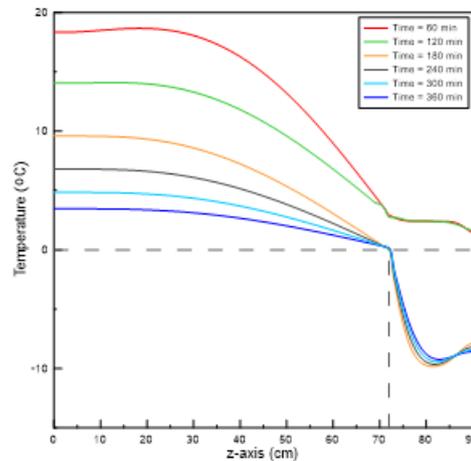

Fig.4 Temperature distribution through z-axis, with value of r = 0 at different intervals time
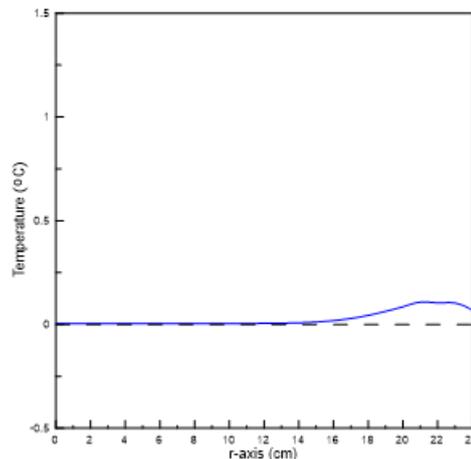

Fig.5 Temperature distribution of phase change location at z = 72 cm, and time = 180 min

Figure (6) to (8) indicate the temporal distribution of temperature through different region in domain of cylindrical enclosure through the solidification process. Following temperature decrease through nine hours of working, in figure (8) the ice growth is expected to be the fastest than the other parts of enclosure especially in the bottom part it's faster. This is due to this layer to be near the heat flux. While the slowest ice was growing in other parts. Because of these parts being the most distant physical point from heat flux. These results confirmed by theoretical work of (Bourdillon *et al*, 2015).
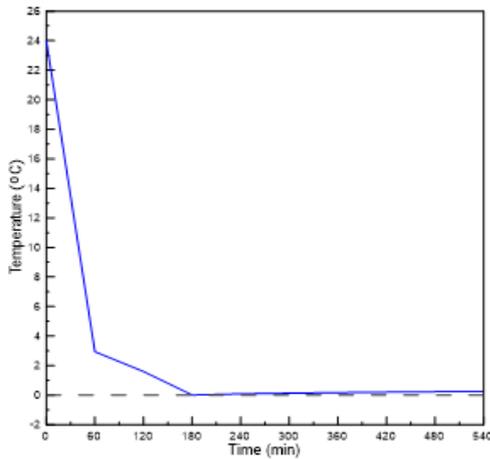
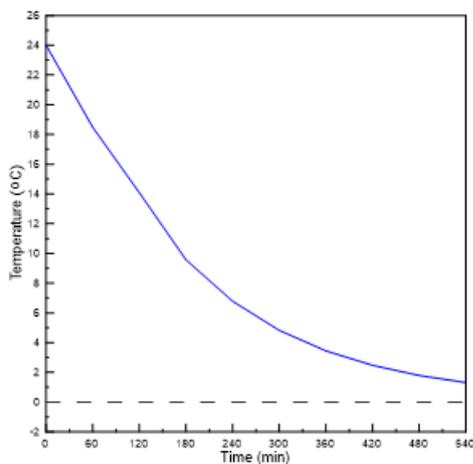**Fig.6** Temporal variation in temperature through center part of cylinder, at r = 0, and z = 72 cm

Fig. 7 Temporal variation in temperature through top part of cylinder, at r = 0, and z = 10 cm

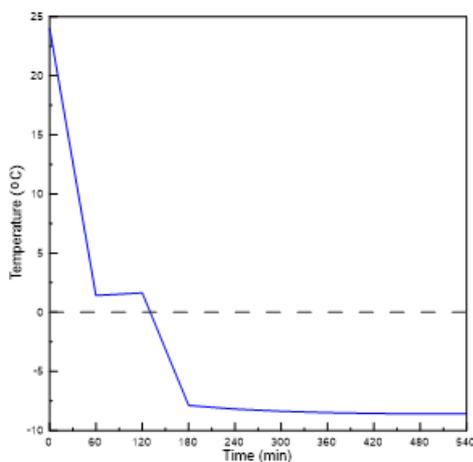

Fig.8 Temporal variation in temperature through bottom part of cylinder at r = 12 cm, and z = 90 cm

Figure (9) describes the isothermal contour map of temperature distribution of phase change phenomenon through solidification process at time of 180 minutes. It has been described the liquid phase temperature in top

part of enclosure and explains how the temperature reduction in down layer through release the heat by down heat flux.

These values of temperature Variable from 9.1 °C at the top layer to 1.05 °C at layer equal 20 cm. The interface line of phase change pointed at layer 18 cm when the water reaches the freezing temperature 0 °C. In this simulation the values of temperature interface line which was about 0.01 °C. A water does not immediately being to freeze when it reaches the phase change temperature, but continue to fall and approach the surrounding temperature of heat flux. Then, solidification of liquid appears after this stage requires the removal of water latent heat and the structuring of atoms into more stable lattice positions as mentioned by (Muhieddine *et al*, 2009).
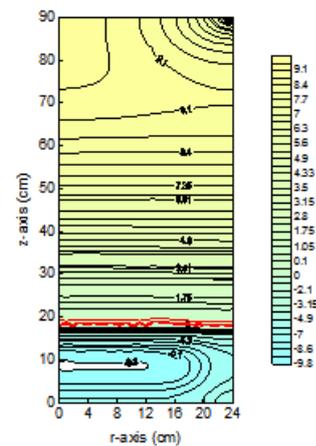

Fig.9 Isothermal contour map of temperature distribution through solidification process at time = 180 min

Conclusions

1) Mathematical models was predicted for solidification process depending upon assumption of the position of the heat flux from the down. This models was simulated numerically by using ADI algorithm. This method gave more reliable results and damping the oscillation errors than other methods with a long computing time.
2) ADI algorithm was used to dominate the phase change phenomenon by a new assumption of moving boundary condition, which was fixed as a prediction distance in the domain of enclosure with time. That was called interface line where the liquid phase jumping to solid phase through release the latent heat energy of water. This interface line moving with time.
3) It was proved that the phase change happens at 18 cm from the down of enclosure, i.e. where the heat flux fixing, and starting after 180 minutes.

Nomenclature

c_{pL}	Specific heat capacity of liquid at constant pressure	$J/kg.^oC$
c_{pS}	Specific heat capacity of liquid at constant pressure	$J/kg.^oC$
k_L	Thermal conductivity of liquid phase........	$W/m.^oC$
V_*	Velocity of interface.........	m/s
t	Time......	s
α_L	Thermal diffusivity of liquid phase.......	m^2/s
α_S	Thermal diffusivity of solid phase...	m^2/s
ρ_L	Density of liquid phase	kg/m^3
ρ_S	Density of solid phase........	kg/m^3
$\delta(t)$	Location of solid-liquid interface........	m
Δr	Increment distance through r-axis...	cm
Δz	Increment distance through z-axis...	cm
λ ,	Convergent	-
$\lambda 1$	Convergent	-

References

Tszeng, T., Im, Y.T., and Yobayashi.(1989). Thermal Analysis of Solidification by the Temperature Recovery Method. International Journal Machine Tool Manufacturing, PP.197-120, No. 1, Vol. 29.

Eames, W., and Adref, K.T.(2002). Freezing and Melting of Water in Spherical Enclosure of the type used in thermal (Ice) storage System. Journal Appl. Thermal Eng. PP. 733-745, Vol. 22.

Michalek, T., and Kowaleski, T.A.(2003). Simulation of the Water Freezing process. Numerical benchmarks, Task Quarterly Vol. 7, No. 3, pp. 389-408.

Ismail, K., Henriquez, J.R., and Dasilva, T.M.(2003). A parametric Study on Ice Formation Inside a Spherical Capsule. International Journal of Thermal Sci., PP. 881-887, Vol. 42.

Stampa. C.S, and Nieckele. A.O.(2004). Numerical Analysis of Indirect Ice Storage Systems Performance. Proceeding of the 10 th Barazilian Congress of Thermal Sciences and Engineering –ENCIT, Braz. Soc. Of Mechanical Sciences and Engineering –ABCM. Riode Janerio, Brazil, Nov. 29-Dec.03.

Alawadhi, E.M.(2004). Solidification Process with Free Convection Process with Free Convection in a Circular Enclosure. ANSYS User Conference, ANSYS Inc.

Alrmah. M. (2005). Numerical Investigation of Solidification. M.Sc. Thesis, Middle East Technical University.

Buyruk, E., Fertemi, A., and Sonmez, N.(2009). Numerical Investigation for Solidification around Various Cylinder Geometries. Journal of Scientific and Industrial Research, PP. 122-129, Vol. 68.

Ezan. A.M, Erek. A, and Dincer. I.(2011). A study on the Importance of Natural Convection during Solidification in Rectangular Geometry. Journal of Heat Transfer ASME, Vol. 133, PP. 10230-10239.

Karlekar, B.V., and Desmond, R.M.(1982). Heat Transfer. Book, second edition, west publishing company, USA.

Adams, j.A., and Rogers, D.F.(1973). Computer Aided Heat Transfer Analysis. Book published by Mc Graw-Hill, Kogakasha Ltd, Tokyo.

Anderson, D.A., Tannehill, j.c., and Pletcher, R.H.(1984). Computational Fluid Mechanics and Heat Transfer. Book, Mc Graw-Hill.

Alwan A.A.(2002). Modeling of Thermal History of Solid materials Processed by Laser., ph.D Thesis, department of mechanical engineering, University of technology.

Scanlon. T. J, and Stickland .M.T.(2004). Numerical Analysis of Buoyancy Driven Melting and Freezing. International Journal of Heat and Mass Transfer, Vol.47, PP. 429-436.

Ulvrova, M., Labrosse, S.,Coltice, N., Raback, p. and Tackley, p.j.(2012). Numerical Modeling of Convection Interacting with a Melting and Solidification Front: Application to the Thermal Evolution of the Basal Magma Occan . J.physics of the earth and planetary, Interior 206-207, pp.51-66.

Bourdillon. A.C, Verdin. P.G, and Thompson .C.P.(2015). Numerical Simulation of Water Freezing Processes in Cavities and Cylindrical Enclosure. Journal Applied Thermal Engineering, Vol. 75, PP. 839-855.

Muhieddine. M, Canot . E, and March. R.(2009). Various Approaches for Solving Problems in Heat Conduction with Phase Change. International Journal on Finite Volumes, Vol. 6, No.1, PP. 1-19.